Journal of Pharmacokinetics and Pharmacodynamics (2022) 49:493–510
https://doi.org/10.1007/s10928-022-09822-y

REVIEW PAPER

Pharmacodynamic model of slow reversible binding and its applications in pharmacokinetic/pharmacodynamic modeling: review and tutorial

Tianjing Ren[1] · Xu Zhu[2] · Natalie M. Jusko[3] · Wojciech Krzyzanski[1] · William J. Jusko[1]

Received: 7 June 2022 / Accepted: 12 August 2022 / Published online: 30 August 2022

Abstract

Therapeutic responses of most drugs are initiated by the rate and degree of binding to their receptors or targets. The law of mass action describes the rate of drug-receptor complex association (k_{on}) and dissociation (k_{off}) where the ratio k_{off}/k_{on} is the equilibrium dissociation constant (K_d). Drugs with slow reversible binding (SRB) often demonstrate delayed onset and prolonged pharmacodynamic effects. This report reviews evidence for drugs with SRB features, describes previous pharmacokinetic/pharmacodynamic (PK/PD) modeling efforts of several such drugs, provides a tutorial on the mathematics and properties of SRB models, demonstrates applications of SRB models to additional compounds, and compares PK/PD fittings of SRB with other mechanistic models. We identified and summarized 52 drugs with in vitro-confirmed SRB from a PubMed literature search. Simulations with a SRB model and observed PK/PD profiles showed delayed and prolonged responses and that increasing doses/k_{on} or decreasing k_{off} led to greater expected maximum effects and a longer duration of effects. Recession slopes for return of responses to baseline after single doses were nearly linear with an inflection point that approaches a limiting value at larger doses. The SRB model newly captured literature data for the antihypertensive effects of candesartan and antiallergic effects of noberastine. Their PD profiles could also be fitted with indirect response and biophase models with minimal differences. The applicability of SRB models is probably commonplace, but underappreciated, owing to the need for in vitro confirmation of binding kinetics and the similarity of PK/PD profiles to models with other mechanistic determinants.

✉ William J. Jusko
wjjusko@buffalo.edu

[1] Department of Pharmaceutical Sciences, School of Pharmacy and Pharmaceutical Sciences, State University of New York at Buffalo, 370 Pharmacy Building, Buffalo, NY 14214-8033, USA

[2] Novartis Institutes for BioMedical Research, Cambridge, MA 02139, USA

[3] Department of Pharmaceutical Sciences, College of Pharmacy, University of Michigan, Ann Arbor, MI 48109, USA

Graphical abstract

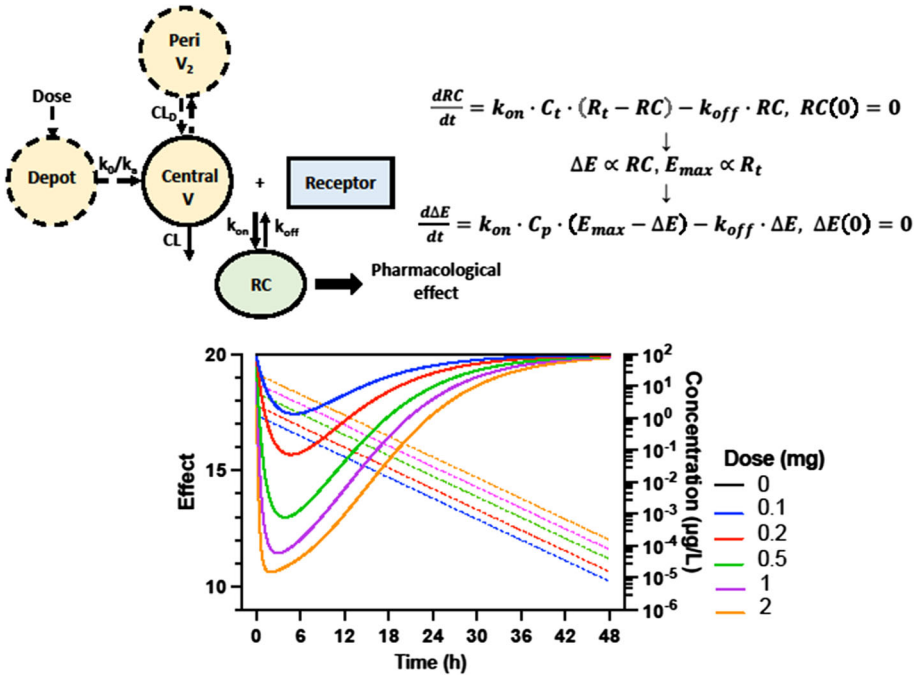

Keywords Slow reversible binding · Pharmacodynamics · Mathematical modeling · Receptor binding kinetics · Indirect response models · Biophase models

Introduction

The pharmacological responses of most drugs are initiated by binding to its receptor or target. To translate the receptor binding into clinical outcomes, many factors need to be considered: drug concentrations at the target site, type of drug-receptor interaction, and receptor activation and transduction processes [1]. The term receptor or target here represents any biological entity that interacts with a drug, including enzymes, ion channels, carrier transporters, DNA, and structures in the nucleus producing ensuing biological responses. Most of the time, binding events occur rapidly so that the receptor-bound drug complex is in constant equilibrium with the free drug at the effect site. In this case, drug-receptor interaction is quantified by receptor affinity and IC_{50}, K_i, or K_d values determined from affinity-based measurements can be used to provide insight into the drug potency, which is also known as the drug thermodynamic selectivity [2]. However, when drug-receptor interaction does not equilibrate instantly, binding kinetics should be considered in accounting for the time-dependent changes in receptor engagement. Various conditions can cause the lack of and variability in equilibration, such as limited accessibility of the receptor binding site, limited conformational flexibility of the receptor, and hydrogen bonds for drug-receptor interaction being shielded by surrounding hydrophobic regions [3]. Under these circumstances, drug efficacy is influenced by the association rate constant (k_{on}), which primarily governes the time for drug to bind to the receptor, and the dissociation rate constant (k_{off}), which mainly determines the duration of receptor occupancy. Thus, even for drugs with similar IC_{50} values for their targets, if their k_{on} and k_{off} values differ, they may still have different response profiles, which is known as kinetic selectivity [2].

For drugs with Slow Reversible Binding (SRB), the duration of drug action can be determined by the dissociation half-life ($0.693/k_{off}$) or residence time ($1/k_{off}$) in addition to its pharmacokinetics. Drug dissociation half-lives can vary from seconds to hours or even days. Long dissociation half-lives often result in prolonged drug action and maximized efficacy [4, 5]. For example, tiotropium is an inhaled long-acting muscarinic acetylcholine receptor antagonist in the management of chronic obstructive pulmonary disease [6]. In a radioligand binding study, tiotropium showed slow dissociation kinetics to human muscarinic receptors with a dissociation half-life of 7.7 h, which is longer than the older antimuscarinic ipratropium

(0.17 h) [7]. The SRB of tiotropium explains its long duration of action of 24 h, compared to less than 6 h for ipratropium [7]. This allows less frequent administration and higher trough efficacy for tiotropium than ipratropium [8]. Compared to fast kinetic drugs, drugs with SRB may be more vulnerable to target-based toxicity. This can be evidenced with antipsychotic agents with different k_{off} from D_2 dopamine receptors. Typical antipsychotic agents, such as nemonapirde, spiperone, and haloperidol, have high affinities to D_2 receptors with long dissociation half-lives (5.92 h, 3.33 h, and 0.67 h, respectively), and are often associated with severe extrapyramidal motor side effects and prolactin elevation [9]. Atypical antipsychotic agents such as clozapine and quetiapine, however, are free from these side effects and show less D_2 receptor affinity with dissociation half-lives less than 0.5 min. This may be explained by the fact that when endogenous dopamine increases, drugs like clozapine can rapidly dissociate from the receptor to provide more access to the dopamine surge and thereby reduce the chance of extrapyramidal side effects and prolactin elevation [9]. Thus, drug binding kinetics, especially for those with slow dissociation, can shape the dose–response relationship by influencing the efficacy, duration of action, and safety [1, 10].

The concept of SRB was noticed by Fuseau and Sheiner in 1984, where nonequilibrium between the drug concentration at the effect site and receptor was considered as a violation of the assumption of an effect compartment model [11]. In 1996, Shimada et al. applied a SRB model to delineate the antihypertensive effects of eight calcium channel blockers [12]. These drugs exhibited long-lasting antihypertensive effects compared to their short plasma elimination half-lives. The delay between plasma concentrations and effects usually produced counterclockwise hysteresis. The delayed effects were captured by incorporating drug association and dissociation rates in the "ion-channel binding model" under the assumption that the pharmacological effect was directly proportional to the concentration of the drug-receptor complex. In addition to the model fitting, the estimated K_d values (ratio of k_{off} /k_{on}) were well correlated with those obtained from in vitro binding studies.

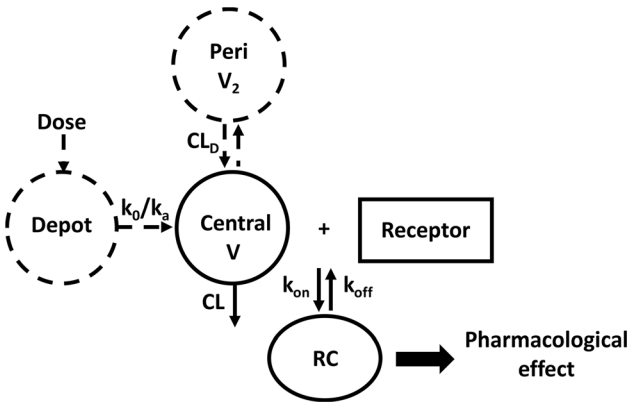

Fig. 1 Structure of the SRB model with general PK compartments and receptor binding. Compartments and processes with broken lines are used when needed

The implications of binding kinetics in drug discovery and lead optimization have been partly reviewed previously [2, 4, 5, 13, 14]. Copeland and Swinney both addressed the importance of obtaining these rate constants as they can provide additional insights on drug-target potency compared to traditional affinity parameters [5, 13]. Drugs with different dissociation half-lives were pointed out to demonstrate the relation of dissociation rate and drug efficacy [4, 5, 13]. Dahl et al. examined the combined effect of PK and binding kinetics on the duration of drug efficacy [14]. Most drugs have a longer elimination half-life than k_{off} half-life.

This report reviews and evaluates PK/PD models of SRB. We provide a review of the literature on drugs with SRB. Since drugs with target-mediated drug disposition (TMDD) demonstrate much more complex PK/PD, they were not included in the current review. A basic SRB model is provided with mathematical derivations of key graphical properties and simulations with signature profiles to describe the effects of dose, k_{on}, k_{off}, E_{max} and elimination rate constant (k_{el}) values on response patterns. Additional demonstrations of model applications to two drugs and their effects illustrate principles of data analysis. Finally, a comparison of the SRB with other basic mechanistic models is provided.

Theoretical

The SRB model (Fig. 1) is based on the classical receptor occupancy theory and the law of mass action [15] with the assumption that the effect of drug (ΔE) is proportional and directly linked to the concentration of the drug-receptor complex (RC). In addition, the model assumes that the delay of response is due to the rate of drug binding to (k_{on}) or dissociating from (k_{off}) the receptors. The total number of receptors (R_t) is assumed to remain constant. The model also assumes that drug concentration at the target site (C_t) is proportional to the plasma drug concentration (C_p) and is in excess compared to receptor concentration.

Accordingly, the rate of change of RC is:

$$\frac{dRC}{dt} = k_{on} \cdot C_t \cdot (R_t - RC) - k_{off} \cdot RC \quad (1)$$

with an initial condition of

$$RC(0) = 0 \quad (2)$$

where R_t is the total receptor content, C_t is the free drug concentration at the target site, k_{on} is a second-order association constant, and k_{off} is a first-order dissociation constant. Free receptors (R) are equal to R_t–RC.

Since the pharmacological effect of drug is assumed to be proportional to the RC concentration, C_t is proportional to the plasma drug concentration (C_p), and the maximum effect (E_{max}) is obtained at $RC = R_t$. The relationship between drug effect and C_p can be defined as:

$$\frac{d\Delta E}{dt} = k_{on} \cdot C_p \cdot (E_{max} - E) - k_{off} \cdot \Delta E \tag{3}$$

with an initial condition of

$$\Delta E(0) = 0 \tag{4}$$

Thus drug effect as $\Delta E/E_{max}$ corresponds to receptor occupancy (RC/R_t). This assumes that the drug is a full agonist. If the mechanism is for a partial agonist or a system with spare receptors, there may exist a more complex proportionality.

When the effect reaches its peak, $\frac{dE}{dt} = 0$, the observed maximum effect (ΔE_m) can be expressed as:

$$\Delta E_m = \frac{k_{on} \cdot E_{max}}{k_{on} + k_{off}/C_m} \tag{5}$$

where C_m is the plasma concentration when ΔE_m is reached ($C_m > 0$). Since the equilibrium dissociation constant (K_d) = k_{off}/k_{on}, Eq. 5 can be rearranged as:

$$\Delta E_m = \frac{E_{max}}{1 + K_d/C_m} \tag{6}$$

Therefore, at a high dose level, C_m is high, which leads to ΔE_m closer to E_{max}. If $C_m >> K_d$, then $\Delta E_m = E_{max}$.

Pharmacodynamic parameter estimations

The following study design is advisable to fully illustrate a PK/PD model of SRB for PD parameter estimation: (1) drug is administered at two or more dose levels; (2) one of the doses should lead to C_{max} much higher than K_d (around 10 times higher); (3) the baseline and/or placebo effects over time should be evident and constant.

Based on Eq. 6, the initial estimation of E_{max} can be obtained from the peak effect at the highest dose.

To obtain the initial estimation of k_{on}, the initial slope (S_I) from the effect versus time curve can be obtained. Since at the initial phase,

$$\frac{d\Delta E}{dt} \; or \; S_1 \cdot \rightarrow k_{on} \cdots C \cdots E_{\max} \cdot \cdots \cdot as \cdot \Delta E \cdot \rightarrow \cdot 0 \tag{7}$$

Using the concentration at the midpoint of the slope (C_{mid}), k_{on} can be obtained as

$$k_{on} \rightarrow \frac{S_I}{C_{mid} \cdot E_{max}} \; as \; \Delta E \rightarrow 0 \tag{8}$$

Based on Eq. 5, an initial estimation of k_{off} can be obtained from the ΔE_m at a dose other than the highest dose, with C_m substituted by the maximum or initial plasma concentration (C_{max} or C_0):

$$k_{off} \rightarrow k_{on} \cdot C_{max/0} \cdot \left(\frac{E_{max}}{\Delta E_m} - 1\right) \tag{9}$$

Due to the non-linearity and time-dependency of the SRB model, the final parameters should be obtained based on fitting the PK/PD model equations using nonlinear least-squares regression analysis.

Methods

Data

Data from the literature were used in the present report. A literature search was performed in PubMed using the keywords "((slow binding kinetics) OR (slow dissociation)) AND (drug)". In addition, references from published articles were traced. The mean values of PK/PD data from the publications were digitalized by WebPlotDigitizer (Version 4.5, https://automeris.io/WebPlotDigitizer). Thus, the estimated PK/PD parameters should be considered approximate.

Data analysis

The PK and PK/PD data were analyzed sequentially. The mean values of the plasma concentrations were first fitted to an appropriate PK model. The PK parameters were then fixed to obtain the plasma concentrations that drive the PD. The PD data were then fitted with the SRB model (Eqs. 3 and 4) to obtain k_{on}, k_{off}, and E_{max}. All data fitting and simulations were performed in NONMEM, version 7.4.1 (Sample model code is provided in Supplemental Materials). The proportional error model and the first-order conditional estimation method with interaction (FOCEI) were used. No interindividual variability was considered since mean values were used. The goodness-of-fit was assessed by the Akaike Information Criterion (AIC), residual error, precision (CV%) of the parameters, and visual check of the fitted curves.

Table 1 Compilation of drugs with slow binding kinetics and their in vitro binding kinetics and efficacy parameters

Class/target	Drug	k_{on} (L/μg·h)	k_{off} (/h)	k_{off} $t_{1/2}$* (h)	K_d (ug/L)	IC_{50}/K_i (ug/L)	*Plasma* $t_{1/2}$ (h)	Ref
Sartans/angiotensin II receptor	Candesartan	3.72	0.213	3.25	0.057	0.21	3.5–4	[18, 39, 60]
			0.347	2				[34]
	EXP-3174		1.39	0.5		0.45	5–10	[35, 60, 61]
	Irbesartan	7.47	2.48	0.28	0.72	0.83	11–18	[35, 60, 61]
	Valsartan	5.40	2.48	0.28	0.46	0.56	6–10	[36, 61]
	Telmisartan	1315	1.42	0.49	0.0011	1.34	21–38	[19, 61]
	Olmesartan	11.33	0.576	1.2	0.051	0.24	14–16	[19, 62]
Antihistamines/histamine H1 receptor	Levocetirizine	0.401	0.3	2.31	0.845	1.23	5.5–8.5	[43, 46]
		0.19	0.433	1.6	2.34	3.09		[21]
	Fexofenadine	0.144	0.66	1.03	4.6	5.02	14.4	[43, 46, 63]
	Desloratadine	2.12	< 0.116	> 6	0.466		3.6–12	[43, 64]
		4.83	0.375	1.85	0.098	0.25		[21]
	Olopatadine	0.32	0.354	1.96	1.10	0.27	2.9–3.4	[21, 65]
	Acrivastine	0.10	3.90	0.18	34.84	21.98	1.4–3.1	[21, 43]
	Noberastine		0.252	2.75		0.047	15	[44, 45]
	Astemizole		< 0.462	> 1.5		0.092	20–24	[44, 45]
	Mequitazine		< 0.462	> 1.5		0.094	45.5	[45, 66]
	Terfenadine		0.189	3.67		2.08	4.5	[17, 45]
		1.27	1.14	0.61	0.90	0.94		[46]
	Cetirizine		0.320	2.17		4.67	7–11	[43, 45]
						2.45		[46]
Anticholinergic bronchodilators /M3 muscarinic receptor	Ipratropium bromide	87.2	4.2	0.165	0.065	0.072	3.2–3.8	[7, 67]
	Tiotropium	20.1	0.09	7.7	0.0038	0.0038	120–144	[7, 68]
			0.020	34.7				[5]
Calcium channel blocker/calcium channel	Amlodipine		0.541	1.28			40–60	[5, 69]
Renin inhibitor/renin	Aliskiren	2.61	0.396	1.75	0.152	0.073	40	[70, 71]
Narcotic analgesics/μ-opioid receptor	Buprenorphine	0.473	0.250	2.77	0.528		3–40	[72, 73]
Antiemetic/neurokinin-1 receptor	Aprepitant	31.44	0.312	2.57	0.010		7.4–9.8	[74, 75]
Antiviral/HIV-1 protease	Darunavir	14.46	0.0028	247	0.00022		15	[16, 76]
	Atazanavir	1.94	0.504	1.4	0.254		6.74	[16, 77]
	Maraviroc	1.19	0.043	16.0	0.036		16	[53, 78]
	Oseltamivir	3.34	1.26	0.55	0.375		1–3	[23, 79]
		3.11	0.684	1	0.219			[23]
	Nelfinavir	0.70	0.90	0.78	1.86		3.5–5	[16, 80]
	Lopinavir	4.92	0.576	1.19	0.119		6.4	[16, 81]
	Saquinavir	0.75	0.54	1.28	0.805		2.9	[16, 82]
	Tipranavir	1.23	0.396	1.75	0.287		6	[16, 83]
Antiviral/ HCV nonstructural protease (NS3)	Telaprevir	0.012	0.354	1.96	29.5	59	5.6	[84, 85]
	Boceprevir	0.016	0.161	4.3	10.4	20.8	3.4	[84, 86]
Antiviral/ HIV integrase enzyme	Dolutegravir		0.0098	71			13–14	[17, 87]
	Raltegravir		0.079	8.8			7–12	[17, 88]
	Elvitegravir		0.257	2.7			9.5	[17, 89]
Anticancer/epidermal growth factor receptor (EGFR)	Lapatinib		0.139	5		1.74	24	[90, 91]

Table 1 (continued)

Class/target	Drug	k_{on} (L/μg·h)	k_{off} (/h)	k_{off} $t_{1/2}$* (h)	K_d (ug/L)	IC_{50}/K_i (ug/L)	*Plasma* $t_{1/2}$ (h)	Ref
Anticancer/heat shock protein 90 (Hsp90)	Geldanamycin	0.027	0.15	4.62	5.6			[52]
Anticancer/adenosine deaminase (ADA)	Deoxycoformycin	32.3	0.017	40	0.00054		4.9–6.2	[92, 93]
Antidiabetic/dipeptidyl peptidase IV (DPP4)	Saxagliptin	1.60	0.198	3.5	0.12	0.11	6.7	[94, 95]
		5.25	0.83	0.83	0.16			[96]
	5-hydroxy saxagliptin	0.76	1.80	0.38	2.37		8.1	[95, 96]
Antipsychotic/D_2 dopamine receptor	Nemonapride	1640	0.12	5.92	0.000073	0.0097		[9]
	Spiperone	4385	0.18	3.33	0.000041	0.04		[9]
	Haloperidol	6608	1.02	0.67	0.00015	0.26	14.5–504	[9, 97]
	Sertindole	11,308	0.84	0.78	0.000074	0.53	53–102	[9, 98]
	Chlorpromazine	12,532	1.2	0.58	0.000096	0.41	11.1	[9, 99]
	Aripiprazole	25.5	1.34	0.52	0.053	0.051	75	[22, 100]
Gonadotropin-releasing hormone (GnRH) antagonists/GnRH receptor	Sufugolix	10.8	0.27	2.8	0.033		67.1–78.7	[101, 102]
	NBI 42,902	11.3	0.16	4.3	0.014		2.7–4.8	[103, 104]
Antiarrhythmics/Na^+ K^+ ATPase enzyme	Digoxin		0.9	0.77		117	26–45	[105–107]
Prostaglandin D_2 receptor 2 (DP2) antagonists/ DP2 receptor	Fevipiprant	6.33	2.88	0.24	0.45		19–20	[108, 109]
Antigout/xanthine oxidase	Allopurinol	1.62	0.14	5	0.086		23	[92, 110]
Antibiotics/ribosome complex, *E. coli*	Josamycin	0.14	0.65	1.07	4.55		1–2	[111, 112]

*Dissociation half-life (k_{off} $t_{1/2}$) = 0.693/k_{off}

Results

Literature review of drugs with slow binding kinetics

Literature search using PubMed resulted in 3443 articles (last accessed in April 2022). Although there is no clear demarcation between fast and slow binding kinetics, drugs with dissociation half-lives longer than 10 min (0.17 h) are considered SRB drugs in the current report and their in vitro binding kinetics, efficacy parameters, and plasma elimination half-lives are summarized in Table 1. These drugs have a variety of therapeutic indications with many of them from sartans, antihistamines, and antivirals. Several drugs demonstrated extremely long dissociation half-lives, such as darunavir (247 h) and dolutegravir (71 h), which explains their potent activities [16, 17]. Many slow binding drugs have long elimination half-lives, which was observed by Dahl et al. [14].

Sources of binding parameters

The drug dissociation rates for these drugs are generally determined by preincubation of radiolabeled drugs with receptors followed by measuring the time-course of the receptor binding under wash-out conditions [18]. The wash-out medium is usually supplied with an excess of unlabeled competitive ligands to replace the binding of radiolabeled drugs to the receptors. The k_{off} can be obtained by fitting the percentage of receptor binding versus time (t) plot as:

$$Receptor\ binding(\%) = e^{-k_{off} \cdot t} \tag{10}$$

Association rates of drugs can be directly measured by the time-course of binding of radiolabeled drugs to the receptors [19]. The percentage receptor binding versus time curve can be first fitted by:

$$Receptor\ binding(\%) = 1 - e^{-k_{obs} \cdot t} \tag{11}$$

to obtain the pseudo-first-order rate constant (k_{obs}). Then k_{on} can then be obtained based on:

$$k_{obs} = k_{on} \cdot [D] + k_{off} \tag{12}$$

where $[D]$ is the radiolabeled drug concentration used for measuring receptor binding. The k_{on} can also be determined in competitive association experiments, where only unlabeled drugs are required to co-incubate with competitive radiolabeled ligands using the Motulsky–Mahan model [20]. Several antihistamines, muscarinic receptor

Table 2 Drugs with applications of slow reversible binding models

Drug	Target	Subject	PD measurement	Ref
Nicardipine, nifedipine, nilvadipine, benidipine, manidipine, barnidipine, nitrendipine, efonidipine	Calcium channel	Human	Change in systolic blood pressure	[12]
Digoxin	Na^+ K^+ ATPase	Human	Change in electromechanical systole corrected for heart rate	[24]
H 335/25	H^+ K^+ ATPase	Dog and human	Gastric acid secretion	[25]
AR-HO47108 (P), AR-HO47116 (M)	H^+ K^+ ATPase	Dog	Gastric acid secretion	[26]
Buprenorphine	μ-opioid receptor	Rat	Tail-flick latency	[27]
			Change in respiratory response	[28]
		Human	Acute pain tolerance	[29]
			Change in respiratory response	[30]

P parent drug, M metabolite

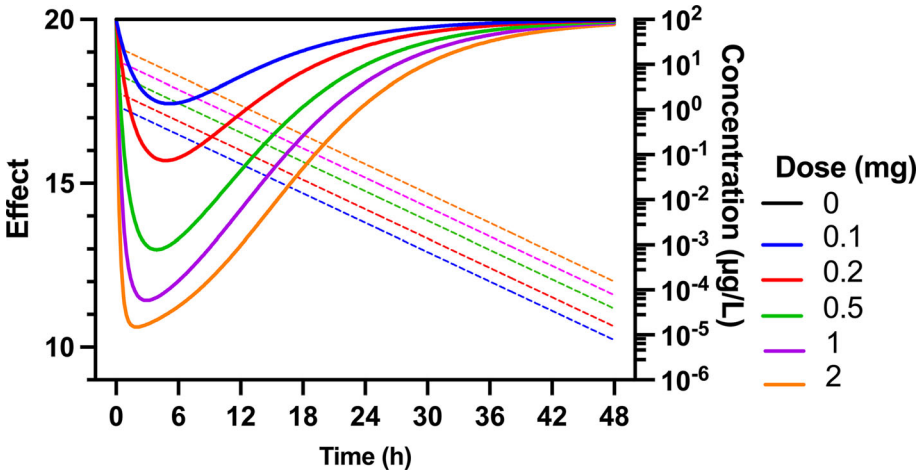

Fig. 2 Simulated PD effects (solid line) of a hypothetical drug with slow reversible binding following single bolus IV administration at doses of 0, 0.1, 0.2, 0.5, 1, and 2 mg. The corresponding PK profiles are shown as dashed lines. Values of CL = 20 L/h, V = 80 L, baseline E_{bl} = 20, E_{max} = 10, k_{on} = 0.125 L/μg·h, and k_{off} = 0.125 /h were used for simulations. The observed effect = $E_{bl} - \Delta E$

antagonists and antipsychotics were measured in this way [7, 21, 22]. Biosensor-based studies or surface plasmon resonance (SPR) technology has been applied to analyze the binding kinetics of antivirals, such as darunavir and atazanavir [16, 23]. It can measure the k_{on} and k_{off} and requires only a small amount of drug without radiolabeling. The drug affinity values (IC_{50}/K_i) summarized in Table 1 are usually higher than K_d, suggesting the underprediction of drug affinity using IC_{50}/K_i values for SRB drugs. Lastly, the value of k_{on} can be determined from $k_{on} = k_{off}/K_d$, once the latter two have been assessed.

Previous SRB modeling

Although many drugs with SRB have been reported, only few studies applied SRB models to describe the PK/PD (Table 2). Besides the application by Shimada et al. [12], the SRB model was applied to describe the inotropic response of digoxin in rats [24]. The model well-captured the digoxin PD after bolus dose and in concentration—clamp experiments. The SRB model was applied in analyzing the anti-secretory effects of several gastric acid pump inhibitors in dogs and humans [25, 26]. One of these, H 335/25, showed rapid onset but delayed effects compared to its PK [25]. The delayed effects were captured by the SRB model and further compared with fittings using biophase and indirect response models. The SRB model was considered superior based on the Akaike Information Criterion. In addition, a SRB model was combined with a biophase model to describe the antinociceptive and respiratory depressant effects of buprenorphine in rats and humans [27–30]. In these studies, concentrations of buprenorphine at an effect site but not in plasma were assumed to form the drug-receptor complex to exert pharmacological effects.

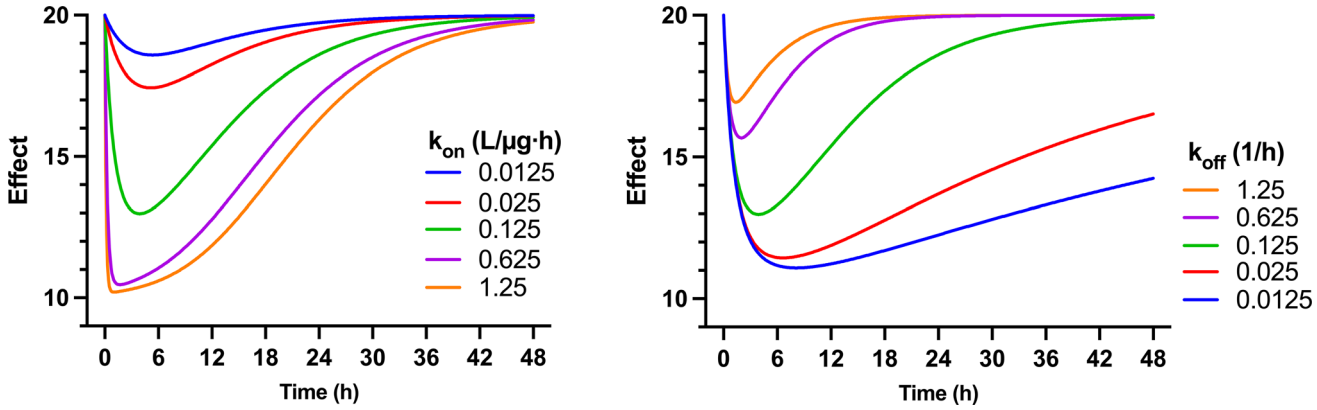

Fig. 3 Simulated PD profiles of drug with indicated k_{on} or k_{off} values following a single bolus IV dose of 0.5 mg. The PK and other parameters used for simulations were the same and held constant as those in Fig. 2. Note that the k_{el} was assumed to be 0.25 1/h

Model simulations

To evaluate the expected properties of the SRB model, the response profiles for a theoretical drug with mono-exponential kinetics and a range of doses were simulated as shown in Fig. 2. The drug is assumed to have clearance (CL) = 20 L/h and volume of distribution (V) = 80 L after bolus intravenous (IV) doses of 0.1, 0.2, 0.5, 1, and 2 mg. The PD parameters of the drug were: baseline E_{bl} = 20, E_{max} = 10, k_{on} = 0.125 L/µg·h, and k_{off} = 0.125 /h. The observed effects $E = E_{bl} - \Delta E$ were generated with no relative standard error.

As doses increased, the overall size of the response profile increased with a rapid initial decline, a plateau at the peak or nadir, and a return to baseline that was nearly linear and parallel at larger doses. The E_m and S_I increased with the time to reach E_m (t_{Em}) shifting to earlier times (at 5.1, 4.8, 3.9, 2.9, and 2 h from low to high doses). Thus, at higher dose levels, a lesser delay in onset of effects is expected.

The explicit formula for area between the baseline and effect curve (ABEC) is:

$$ABEC = \frac{E_{max}}{k_{el}} ln\left(1 + \frac{Dose/V}{K_d}\right) \quad (13)$$

as shown by derivations in the Supplemental Materials.

Thus, ABEC is expected to increase in proportion to E_{max}, $1/k_{el}$, and the log of the dose at higher value This has similar determinants as the ABEC of direct and indirect response models [31, 32]. By substituting C_m with the initial concentration (C_0) of 1.25, 2.5, 6.2, 12.5, and 25 µg/L from 5 doses in Eq. 6, the resulting effects were 4.67, 6.51, 8.38, 9.17, and 9.59, which were close to the E_m of 2.57, 4.31, 7.02, 8.57, and 9.39. Thus, E_m can be obtained based on Eq. 6 with either C_0 or C_{max}.

Response profiles were also generated for a dose of 0.5 mg with changes in k_{on} (0.0125, 0.025, 0.125, 0.625, and 1.25 L/µg·h) or k_{off} (0.0125, 0.025, 0.125, 0.625, and 1.25 /h) as demonstrated in Fig. 3. When k_{on} increased, the E_m and S_I increased with t_{Em} shifting to an earlier time. Decreasing k_{off} led to increase in E_m and a later t_{Em} but without change in S_I. The profiles for the SRB become particularly distinctive when k_{off} is much smaller than k_{el} producing, as expected, a prolonged duration of responses (also see Supplementary Fig. 2).

The effects of E_{max} and k_{el} on the PK/PD profiles for a dose of 0.5 mg were further evaluated. With increased E_{max}, the E_m and S_I increased with the t_{Em} remaining constant (Supplementary Fig. 1). The recession slopes (S_{fp}) were directly proportional to E_{max} values. Decreasing k_{el} (2.5, 1.25, 0.5, 0.05, and 0.025 /h) by changing CL to 200, 100, 20, 4, and 2 L/h resulted in an increased E_m and a later t_{Em} and without changes in S_I values (Supplementary Fig. 2). The recession slopes increased with lower k_{el} but decreased at higher k_{el} values.

The pharmacodynamic profiles of the SRB model showed a single inflection point during the recession phase. The slope at the inflection point (S_{fp}) was derived and is fully determined by the k_{on}, k_{off}, k_{el}, E_{max}, concentration at the inflection point (C_{fp}), and effect at the inflection point (ΔE_{fp}) (Supplementary Materials). However, it was found that C_{fp} approaches a limiting value as the dose becomes very large. This results in a limiting value for S_{fp} so that the recession slopes are parallel at larger doses (Supplementary Fig. 3). In addition, it can be noted that the occurrence of C_{fp} becomes closer to K_d in the effect curve when $k_{off} >> k_{el}$ (Supplementary Fig. 4).

When k_{off} becomes very large, the SRB model will behave like a simple direct effect model as drug-receptor binding essentially equilibrates instantly. The ratio of S_{fp}/k_{off} is an upper bound for the difference between these two models (derivation provided in Supplementary Materials). Thus, after normalizing with the effect, the quotient $(S_{fp}/k_{off})/(E_0 - E_{max})$ can serve as a metric to examine the

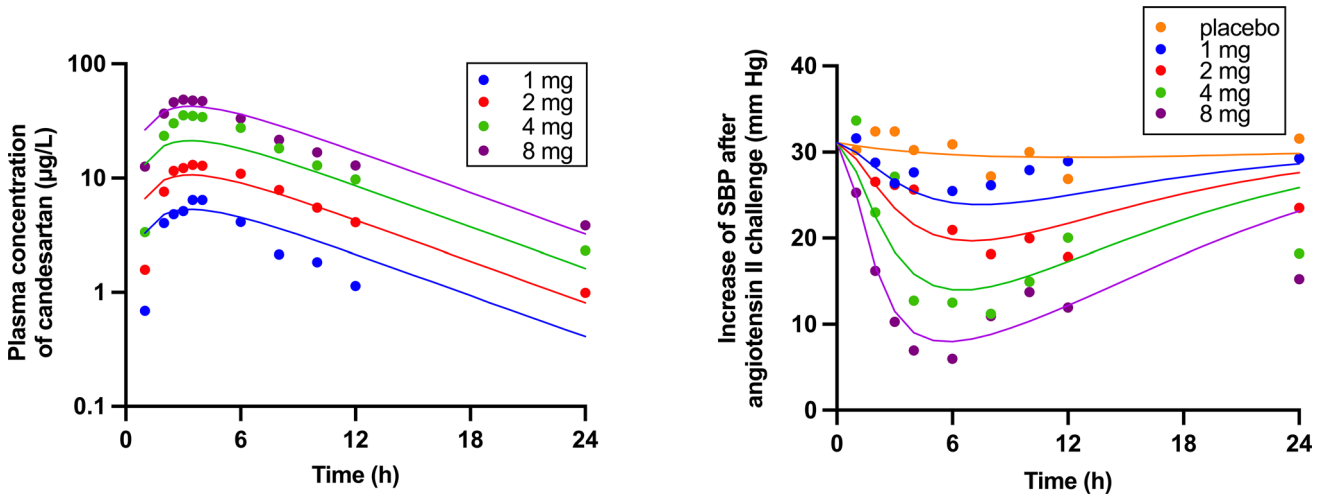

Fig. 4 PK/PD profiles of candesartan on systolic blood pressure (SBP) after single oral administration of either candesartan cilexetil at the indicated doses or placebo in healthy volunteers. A one-compartment PK model with first-order absorption and elimination and SRB model as shown in Fig. 1 was applied. Symbols depict data calculated from Delacrétaz et al. [39], and lines are fitted responses. Parameters are presented in Table 3

Table 3 PK/PD parameters of candesartan effects on systolic blood pressure in humans

Parameters	Units	Definition	Estimate (CV%)
PK			
k_a	1/h	Absorption rate constant	0.54 (6.1)
CL/F	L/h	Clearance	11.8 (10.3)
V/F	L	Volume of distribution	84.3 (11.4)
PD			
k_{on}	L/µg·h	Second-order association rate	0.0142 (12.9)
k_{off}	1/h	First-order dissociation rate	0.277 (62.5)
E_{max}	mm Hg	Maximum effect	33 (25.8)
BASL	mm Hg	Baseline effect	31.1 (fixed)
DREC	mm Hg	Amplitude of placebo effect	4.59 (fixed)
k_{ep}	1/h	Rate of placebo effect	0.0829 (fixed)

Table 4 PK/PD parameters of noberastine effects on histamine induced wheal diameter in humans

Parameters	Units	Definition	Estimate (CV%)
PK			
k_0	mg/h	Absorption rate constant	30 (fixed)
CL/F	L/h	Clearance	258 (7.4)
CL_D/F	L/h	Distribution clearance	177 (10.5)
V/F	L	Central volume of distribution	2150 (1.4)
V_2/F	L	Peripheral volume of distribution	1980 (4.8)
PD			
k_{on}	L/µg·h	Second-order association rate	0.134 (7.3)
k_{off}	1/h	First-order dissociation rate	0.203 (6.9)
E_{max}	cm	Maximum effect	7.61 (1.9)
BASL	cm	Baseline effect	6.9 (2)

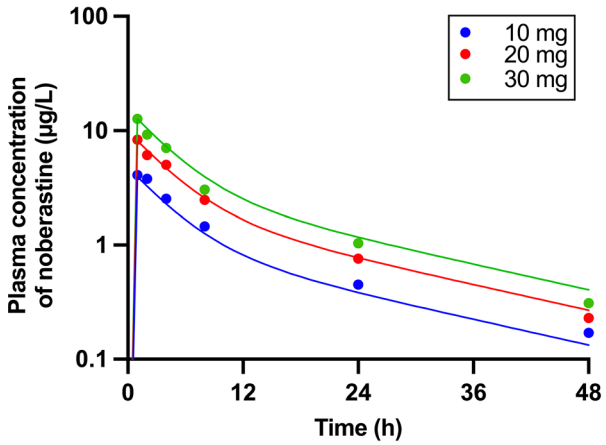

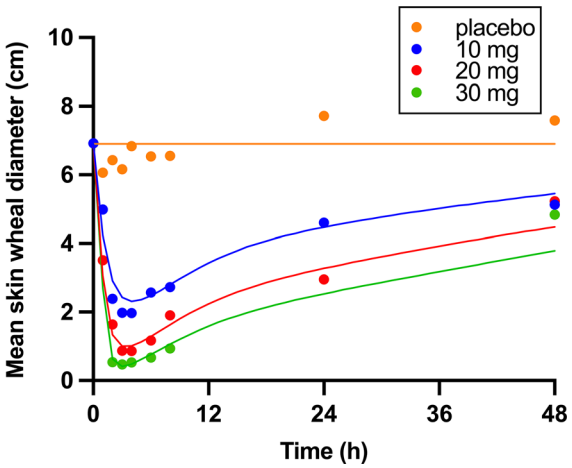

Fig. 5 PK/PD profiles of noberastine on histamine induced wheal diameter after single oral doses as indicated or placebo in healthy volunteers. A two-compartment PK model with zero-order absorption and first-order elimination and SRB model as shown in Fig. 1 was applied. Symbols depict the observed data from Wood-Baker et al. [48], and lines are fitted responses. Parameters are presented in Table 4

convergence of a SRB to a direct effect model (Supplementary Fig. 5). When k_{off} is larger than 4, corresponding to a dissociation half-life shorter than 10 min, $(S_{fp}/k_{off})/(E_0 - E_{max})$ is close to zero, suggesting the convergence of the SRB to the direct effect model. Therefore, the SRB should be considered for drugs with a dissociation half-life longer than 10 min; otherwise, a simple direct effect model can be applied. A consequence of convergence of the SRB model to the simple direct model for large k_{off} is that C_{fp}, ΔE_{fp}, and S_{fp} are converging to the values reported for the latter model elsewhere [33]. Hence, C_{fp} becomes close to K_d, ΔE_{fp} close to $E_{max}/2$ and S_{fp} close to $k_{el} \cdot E_{max}/4$.

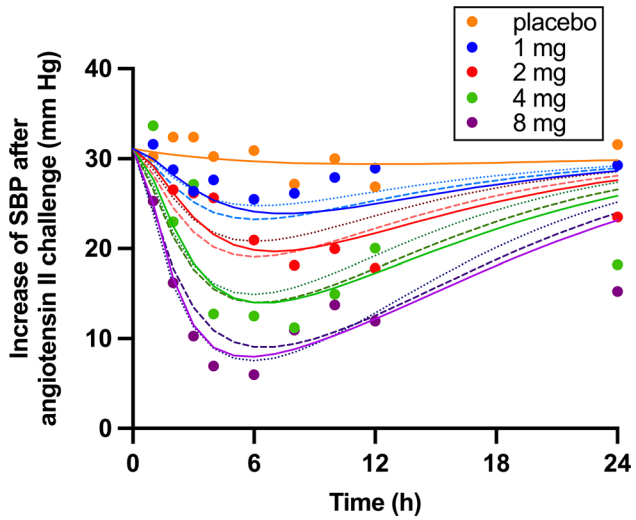

Fig. 6 Model fittings for the effects of candesartan on systolic blood pressure in humans by the slow binding model (solid line), indirect response model I (broken line), and biophase model (dotted line). The data generated from Delacrétaz et al. [36] are shown as solid circles

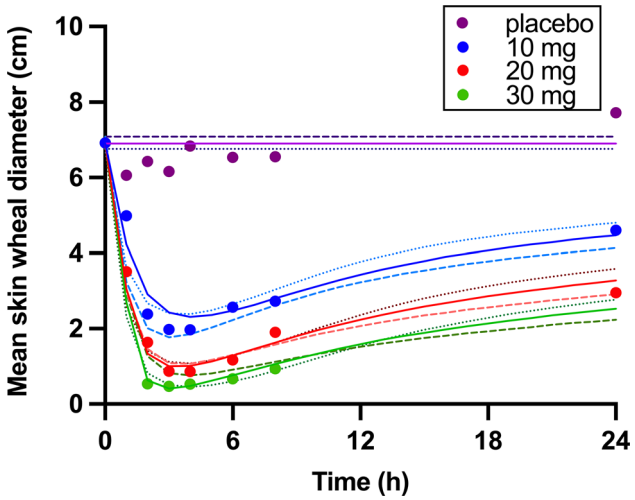

Fig. 7 Model fittings for the effects of noberastine on histamine induced wheal diameter in humans by the slow binding model (solid line), indirect response model I (broken line), and biophase model (dotted line). The observed data from Wood-Baker et al. [44] are shown as solid circles

Clinical PK/PD examples of SRB applications

Sartans

Sartans are orally active angiotensin II receptor type 1 (AT1) antagonists used for the treatment of hypertension and related diseases [34]. A number of sartans are frequently used in clinical therapy, including candesartan, olmesartan, telmisartan, valsartan, irbesartan, and losartan. Although they share a common binding site, their binding kinetics differ, which results in different binding potency and clinical effects. Losartan showed a surmountable antagonism phenomenon in an in vitro study, which is typical

Table 5 Pharmacodynamic parameters of candesartan effects on systolic blood pressure in humans assessed by three models

Parameters	Units	Definition	Slow reversible binding model	Indirect response model I	Biophase model
AIC		Akaike Information Criterion	158.17	168.76	165.87
k_{on}	L/μg·h	Second-order association rate	0.0142 (12.9)	–	–
k_{off}	1/h	First-order dissociation rate	0.277 (62.5)	–	–
k_{out}	1/h	First-order removal rate	–	0.606 (42.1)	–
k_{eo}	1/h	First-order distribution rate	–	–	0.544 (79)
IC_{50} *or* K_d	μg/L	Concentration at half-maximal inhibition/ dissociation constant	19.5	12.9 (6.4)	26.6 (133.1)
I_{max}		Maximal inhibition	–	1 (fixed)	–
E_{max}	mm Hg	Maximal effect	33 (25.8)	–	44 (71.6)
BASL	mm Hg	Baseline effect	31.1 (fixed)	31.1 (fixed)	31.1 (fixed)
DREC	mm Hg	Amplitude of placebo effect	4.59 (fixed)	4.59 (fixed)	4.59 (fixed)
k_{ep}	1/h	Rate of placebo effect	0.0829 (fixed)	0.0829 (fixed)	0.0829 (fixed)
Prop. error		Proportional error	0.159 (19.6)	0.182 (19.2)	0.17 (20.8)

Table 6 Pharmacodynamic parameters of noberastine effects on histamine-induced wheal diameter in humans assessed by three models

Parameters	Units	Definition	Slow reversible binding model	Indirect response model I	Biophase model
AIC		Akaike Information Criterion	–27.4	11.19	–13.1
k_{on}	L/μg·h	Second-order association rate	0.134 (7.3)	–	–
k_{off}	1/h	First-order dissociation rate	0.203 (6.9)	–	–
k_{out}	1/h	First-order removal rate	–	1.17 (15.6)	–
k_{eo}	1/h	First-order distribution rate	–		0.458 (12.6)
IC_{50} *or* K_d	μg/L	Concentration at half-maximal inhibition/ dissociation constant	1.51	0.906 (11.8)	2.12 (7.2)
I_{max}		Maximal inhibition	–	1 (fixed)	–
E_{max}	cm	Maximal effect	7.61 (1.9)	–	8.1 (1.5)
BASL	cm	Baseline effect	6.9 (2)	7.09 (6.1)	6.76 (0.9)
Prop error		Proportional error	0.159 (19.6)	0.22 (24.2)	0.154 (11.4)

for fast-dissociating antagonists [35]. Most sartans, such as candesartan, olmesartan, telmisartan, valsartan, and irbesartan, produced partial depression of the maximal response in the in vitro study, which is known as insurmountable antagonism [19, 34, 36]. Such behaviors are largely due to their slow dissociation from AT1 receptors, especially for candesartan with a dissociation half-life of 3.25 h in the radioligand binding study [18]. Comparison of clinical studies showed that sartans with slow dissociation, such as valsartan, olmsartan and candesartan, had higher maximal effects on blood pressure than losaratan, which has a fast dissociation rate [5].

Candesartan cilexetil (TCV-116) is the esterified prodrug of candesartan and has been approved in many countries to treat hypertension [37]. Absorbed candesartan cilexetil is presumed to be completely metabolized to candesartan to exert pharmacological actions [38]. Delacrétaz et al. evaluated the inhibitory effect of candesartan on blood pressure after oral administration of candesartan cilexetil at 1, 2, 4, and 8 mg in healthy volunteers [39]. At 45 min before candesartan cilexetil or placebo administration, an IV bolus injection of angiotensin II at preestablished doses was given to increase the systolic blood pressure (SBP) by 31.1 mm Hg on average, which was

considered as the baseline response. The plasma concentration of candesartan and change in SBP after drug intake were monitored. The plasma PK of candesartan following four oral doses were captured jointly by a one-compartment model with first-order absorption and elimination (Fig. 4). The PD of candesartan were assessed from the increase of SBP after angiotensin II challenge, which were back-calculated from the percent of baseline response in the published plot using the baseline response (BASL) of 31.1 mm Hg. The responses in the placebo group were described by a modified inverse Bateman function [40, 41]:

$$PLACEBO = BASL - DREC \cdot k_{ep} \cdot t \cdot e^{-kep \cdot t} \quad (14)$$

where *DREC* is the amplitude of placebo effect and *kep* is the rate constant for the associated placebo effect.

The PD effects of candesartan were obtained by:

$$Effect = PLACEBO - \Delta E \quad (15)$$

where ΔE was based on the operation of SRB model (Eqs. 3 and 4). The parameters for describing placebo effects were fixed during the model fitting of PD profiles of candesartan at four dose levels (Fig. 4). The PK and PD parameters after model fitting are listed in Table 3. The estimated k_{on} = 0.0142 L/μg·h (12.9% CV) and E_{max} = 33 mm Hg (25.8% CV) demonstrated reasonable precision. The estimated k_{off} was 0.277 1/h (62.5% CV), which translates to a dissociation half-life of around 2.5 h. This is close to the dissociation half-life of 3.25 h determined in the in vitro study [18].

H_1-Antihistamines

H_1-antihistamines are first-line treatments for allergic rhinoconjunctivitis and urticaria [42]. They target histamine, the major pathogenic mediator of allergic disorders, by binding to H_1-receptors to reduce the constitutive activity of the receptor and block the binding of histamine to the receptor [43]. The first-generation antihistamines, such as chlorpheniramine, diphenhydramine, hydroxyzine, and ketotifen, demonstrated central nervous system (CNS) penetration that resulted in sedation and interference with the cognitive process [43]. The second-generation antihistamines overcome the CNS side effects with improved selectivity and tolerability. These include acrivastine, astemizole, cetirizine, ebastine, levocabastine, mizolastine, noberastine and terfenadine [44]. The in vitro receptor binding studies revealed the slow dissociation from the H_1-receptor for several antihistamines, such as astemizole, cetirizine, fexofenadine, loratadine, levocetirizine, mequitazine, noberastine, and terfenadine [45, 46]. This may contribute to the delayed onset and prolonged pharmacological actions of antihistamines observed in clinical studies [43, 47].

Noberastine is a second-generation non-sedating antihistamine. The PK/PD profiles of noberastine at single oral doses of 10, 20, and 30 mg in healthy volunteers were published by Wood-Baker et al. [48]. The plasma concentrations of noberastine were fitted using a two-compartment model with zero-order absorption and first-order elimination (Fig. 5). The PD responses of noberatine were assessed by the wheal diameters caused by histamine skin prick testing. One hour before drug administration, the baseline skin prick testing was performed to get the baseline wheal diameter. After drug administration, wheal diameters at designated intervals remained at similar levels to baseline in the placebo group and were inhibited in the noberastine treatment groups. Thus, the observed wheal diameters were described by

$$Effect = BASL - \Delta E \quad (16)$$

where BASL was the baseline level and ΔE was based on the operation of SRB model (Eqs. 3 and 4). The parameters after model fitting are listed in Table 4. The zero-absorption rate was fixed to 30 mg/h since the data points in the absorption phase are limited. The PD profiles at all dose levels were well captured by the SRB model with good precision (1.9 to 7.3% CV) (Fig. 5). The dissociation half-life calculated based on the estimated k_{off} of 0.203 1/h was 3.41 h, which is close to the dissociation half-life of 2.75 h measured in an in vitro study [45].

Comparison of SRB model with indirect response and biophase models

In addition to the SRB model, we fitted the PD data of candesartan and noberastine with indirect response model I and the biophase model. The data can be captured by all three models with their fitted curves close to each other (Figs. 6 and 7). The very similar predictions from the three models were also observed for describing the effects of the gastric acid pump inhibitor, H 335/25, by Äbelö et al. [25]. However, one of the noticeable differences between the three models is that the peak or nadir effect is reached earlier with increasing doses for the SRB model; indirect response models exhibit peak or nadir effects later with increasing doses; and biophase models produce the time to peak or nadir effects that are constant for all doses. The PD plots of candesartan and noberastine both demonstrated an earlier nadir at higher doses, suggesting that the SRB model may be more appropriate. In addition, the SRB model showed the lowest AIC with acceptable variability for the two drugs (Tables 5 and 6). The biophase model for candesartan showed the poorest precision of estimated parameters (CV > 71.6%). Therefore, the SRB model was superior to the other two models for the current PK/PD data for candesartan and noberastine. However, the differences

between the three models are minimal. This may also result from the similar plasma elimination rates and dissociation rates for candesartan and noberastine, which will retain the return phase of the PD plots. Even when elimination rate is comparable or slower to the dissociation rate, the time to reach to peak or nadir effect are earlier at higher doses still hold true for SRB model. Thus, high quality data from a wide range of dose levels are required to differentiate the model type in performing fittings.

It is interesting to note that the 50% effective drug concentration values (EC_{50}, IC_{50} *and* K_d) are similar for each drug for the three models. This might be expected since it is the same PK profiles that are driving the same responses.

Discussion

The responses of many drugs with SRB can be described by a simple model based on the law of mass action and classical receptor occupancy theory. This model connects the drug PK and effects by considering the kinetics of receptor association and dissociation. Distinctive signature profiles are produced as compared to some other PD models.

The model of SRB demonstrated delayed onset and prolonged responses as the result of slow binding of the drug to the receptor. Increased doses lead to larger effects with peak or nadir effects shifting to earlier times. The onset slope is related to dose, k_{on} and E_{max} while the recession slope exhibits more complex behavior and approaches to a limiting value determined by k_{el} and E_{max} for higher doses. In addition, the SRB model will behave like simple direct effect model when k_{off} becomes very large. Based on our simulations with k_{el} of 0.25 1/h, the SRB model is generally considered for a drug with dissociation half-life longer than 10 min. However, it is difficult to define a clear cutoff value of k_{off} or k_{on} for SRB drugs based on these simulations as they cannot reflect the universe of possible combinations of the independent variables. Dahl et al. observed that the duration of effect will be most prolonged when k_{off} is slower than *kel* [14], but most drugs have a faster k_{off} as we also show in Table 1.

While ionotropic receptors might be most likely to produce SRB profiles, metabolotropic (G-protein mediated), kinase, and nuclear receptors might produce delayed responses owing to the signaling cascades that follow receptor binding. However, the drugs listed in Table 1 and 2 show interactions with diverse targets including receptors and protease and integrase enzymes.

Proper in vitro experimental conditions are essential to obtain accurate binding kinetic parameters for drugs with SRB. For measuring k_{off}, the wash-out conditions are discerned by whether the fresh medium is used to replace the radiolabeled drug-containing medium and whether an excess amount of unlabeled competitive ligand is supplied [4]. The former condition may not substantially influence k_{off} whereas the latter condition of adding unlabeled ligand can effectively prevent the rebinding of the dissociated drug to the receptor, a phenomenon pervasively found for drugs with slow dissociation that can further prolong the dissociation [4, 49]. In the in vitro dissociation study with candesartan, when unlabeled candesartan is supplied, the dissociation half-life of candesartan decreased from 11.6 h to around 2 h [50]. The acceleration in k_{off} positively correlated with the amount of unlabeled ligand added in the medium, so the addition of an excess amount of unlabeled ligand (usually 100-fold) is required. Alternatively, diluting the radiolabeled drug-containing medium before adding unlabeled ligand to ensure the accuracy of measuring k_{off} is needed [50]. The K_d is sometimes measured as a surrogate of binding kinetics and reflects the affinity of the drug to the receptor. However, K_d must be obtained at equilibrium condition, which may be difficult to achieve for drugs with long dissociation half-lives. Lack of equilibration may result in underpredicting the affinity, so a higher K_d value is obtained [51]. In a saturation binding assay of candesartan, increasing incubation times from 5 to 180 min resulted in decreased apparent K_d from 1 to 0.02 nM, suggesting a lack of equilibration with short incubation time [50]. Similarly, geldanamycin demonstrated a 40-fold decrease in K_d over 24 h incubation time [52]. The K_d of maraviroc obtained in the saturation binding study (0.86 nM) was also higher than the K_d calculated from the ratio of k_{off}/k_{on} (0.071 nM) [53]. Thus, for drugs with SRB, it is better to obtain K_d either from the kinetic parameters k_{off} and k_{on} or from saturation binding studies with sufficient incubation times (5-times the dissociation half-life) [51]. More advanced technology, such as resonance energy transfer (RET) based techniques with fluorescent or bioluminescent energy sources, enables high-throughput binding kinetic assays [54]. Surface plasmon resonance methodology provides a rigorous measurement of binding kinetics [16].

Several assumptions were made in our operation of the SRB model. The most important one is that the drug effect is assumed to be directly linked and proportional to the *RC* concentration. Under this condition, *RC* and R_t concentrations in the classical receptor occupancy theory can be replaced by drug effect and E_{max}. This is more of a simplified scenario as the true relationship between receptor occupancy and response may be of sigmoid shape and other transduction and homeostatic feedback mechanisms may be involved [1]. More complex models with binding kinetics have been reviewed [10]. Another assumption is that the plasma concentration is proportional to the drug

concentration at the target site and is much greater than the receptor concentration. This allows the fraction of drug bound to the receptor to be negligible in relation to the free drug concentration; thus the plasma concentration can be used as a surrogate for free drug concentration and drug PK is not influenced by drug receptor binding. If the concentrations of drug and receptor are comparable, free drug concentrations change during receptor binding, which is a more complex situation known as slow tight-binding [55]. Under this condition, receptor binding may influence the drug PK, which can be described by the TMDD model [56]. This review does not consider drugs and proteins with TMDD properties as both the PK and PD become far more complicated.

The current report showed the application of the SRB model to the antihypertension effects of candesartan and antiallergic effects of noberastine. Their PD effects were well-captured by the SRB model. The dissociation half-lives of the two drugs from the model predictions were close to their in vitro dissociation half-lives [18, 45]. This suggests an opportunity for using the SRB model with in vitro binding kinetic parameters to predict drug responses. However, the predicted K_d for candesartan (19.5 ug/L) is higher than the in vitro measured K_d (5.7 ng/L) [18]. This may be attributed to the extensive plasma protein binding of candesartan (> 99% in humans) [37], which may lead to the true free drug concentrations for receptor binding being much lower than the total plasma concentration. Noberastine also showed an underpredicted K_d of 1.51 ug/L compared to its in vitro K_i of 47 ng/L [45]. Although no plasma protein binding information was found for noberastine, many secondary-generation antihistamines demonstrate high protein binding, which may contribute to in vitro/in vivo differences in affinity [57].

Besides the similarities in shapes and in fitting response profiles, the three basic PK/PD models (as well as direct effect models) share the properties of a *ABEC* that is proportional to log Dose at higher doses and recession slopes that are essentially linear, parallel for higher doses, and determined by the E_{max} (or equivalent) and terminal slope of the PK (k_{el}) or biophase (k_{eo}) constant. Further, the SRB model can be interpreted as an indirect response model with a linear effect on k_{out} when $k_{off} \cdot E_{max} = k_{in}$, $k_{off} = k_{in}$, and $E_{max} = R_o$. This indicates the need for higher doses of drugs in order to discriminate between these models by fitting data. It can be noted that the SRB and biophase models only require fitting of 3 parameters, while full indirect response model models require 4 parameters.

A biophase can be added to the SRB model either for greater mechanistic relevance or to further capture delays between drug concentrations and responses. This was done in investigating the antinociceptive and respiratory depressant effects of buprenorphine in rats and humans by Yassen et al. [27–30], where they showed that adding an effect compartment significantly improved the modeling performance. The biophase delay likely reflects the slow distribution of buprenorphine into or from the brain [29]. Thus, biophase equilibration and receptor binding can both contribute to the delayed and prolonged effects of slow binding drugs. Of course, other pharmacologic complexities may also apply such as turnover of targets, receptor desensitization, more complicated receptor binding kinetics, and nonlinear- or time-dependent transduction processes. When multiple steps are involved in the pharmacological response, such as for some corticosteroid actions, receptor-binding events with k_{off} and k_{on} can be included as an early step in a mRNA/protein/biomarker cascade [58]. In addition, free drug concentrations will often be the preferred substrate for many drugs and receptors. Further, when receptor mechanisms involve partial agonists, spare receptors, or nonlinear transduction the concepts from Black and Leff [59] should be invoked. In essence, our model is simply a basic starting point that can be expanded in many ways.

The SRB model has been introduced and used since 1990s but has been largely overlooked. One possible reason is that other PD models, like indirect response and biophase models, can produce similar profiles as SRB and produce similar K_d, EC_{50} or IC_{50} values. Many slow binding drugs also have long elimination half-lives, which may mask their SRB nature and produce similar profiles as direct effect models. Another reason is the limited availability of the kinetic binding parameters as additional in vitro experiments are required. However, the SRB model should clearly be part of the "toolbox" of pharmacometricians as it is intrinsically mathematically and graphically different from other PD models and might fit data better than with other models. The SRB model illustrated in the present study is a simplified version when binding kinetics are considered as the rate-limiting step for PD effects, but works quite well for many drugs.

Conclusions

The kinetics of SRB have significance in drug action and help shape the clinical outcomes and safety profiles of many drugs. For drugs with slow association or dissociation rates from targets, a simple SRB model can be used to describe delayed drug responses by incorporating drug binding kinetics. To apply the SRB model with better estimation, high quality data from a wide range of doses with rich sampling points and additional confirmation from in vitro experiments are required. However, if only based on drug PD responses, it may be difficult to discern the SRB from indirect response and biophase models. Thus,

mechanistic studies are required to understand the rate-limiting step in affecting the drug responses and to ensure appropriate model selection and application.

Supplementary Information The online version contains supplementary material available at https://doi.org/10.1007/s10928-022-09822-y.

Acknowledgements Supported by a Fellowship for TR from GlaxoSmithKline and by NIH Grant R35-GM131800 for WJJ.

Author contributions Contributed to the study conception and design TR, XZ, WJJ; Conducted literature review: TR, XZ; Performed data analysis: TR, XZ, NMJ, WK; Wrote or contributed to the writing of the manuscript: TR, XZ, WK, WJJ.

Declarations

Conflict of interest The authors declare no conflicts of interest.

References

1. Ploeger BA, van der Graaf PH, Danhof M (2009) Incorporating receptor theory in mechanism-based pharmacokinetic-pharmacodynamic (PK-PD) modeling. Drug Metab Pharmacokinet 24(1):3–15
2. Tonge PJ (2018) Drug–target kinetics in drug discovery. ACS Chem Neurosci 9(1):29–39
3. Pan AC, Borhani DW, Dror RO, Shaw DE (2013) Molecular determinants of drug–receptor binding kinetics. Drug Discov Today 18(13):667–673. https://doi.org/10.1016/j.drudis.2013.02.007
4. Vauquelin G, Charlton SJ (2010) Long-lasting target binding and rebinding as mechanisms to prolong in vivo drug action. Br J Pharmacol 161(3):488–508
5. Swinney DC (2008) Applications of binding kinetics to drug discovery. Pharmaceut Med 22(1):23–34. https://doi.org/10.1007/BF03256679
6. Price D, Sharma A, Cerasoli F (2009) Biochemical properties, pharmacokinetics and pharmacological response of tiotropium in chronic obstructive pulmonary disease patients. Expert Opin Drug Metab Toxicol 5(4):417–424
7. Dowling MR, Charlton SJ (2006) Quantifying the association and dissociation rates of unlabelled antagonists at the muscarinic M3 receptor. Br J Pharmacol 148(7):927–937. https://doi.org/10.1038/sj.bjp.0706819
8. van Noord JA, Smeets JJ, Custers FL, Korducki L, Cornelissen PJ (2002) Pharmacodynamic steady state of tiotropium in patients with chronic obstructive pulmonary disease. Eur Respir J 19(4):639–644. https://doi.org/10.1183/09031936.02.00238002
9. Kapur S, Seeman P (2000) Antipsychotic agents differ in how fast they come off the dopamine D2 receptors Implications for atypical antipsychotic action. J Psychiatry Neurosci 25(2):161–166
10. Daryaee F, Tonge PJ (2019) Pharmacokinetic–pharmacodynamic models that incorporate drug–target binding kinetics. Curr Opin Chem Biol 50:120–127
11. Fuseau E, Sheiner LB (1984) Simultaneous modeling of pharmacokinetics and pharmacodynamics with a nonparametric pharmacodynamic model. Clin Pharmacol Ther. https://doi.org/10.1038/clpt.1984.104
12. Shimada S, Nakajima Y, Yamamoto K, Sawada Y, Iga T (1996) Comparative pharmacodynamics of eight calcium channel blocking agents in Japanese essential hypertensive patients. Biol Pharm Bull 19(3):430–437
13. Copeland RA, Pompliano DL, Meek TD (2006) Drug–target residence time and its implications for lead optimization. Nat Rev Drug Discov 5(9):730–739
14. Dahl G, Akerud T (2013) Pharmacokinetics and the drug–target residence time concept. Drug Discov Today 18(15–16):697–707
15. Ariens EJ (1954) Affinity and intrinsic activity in the theory of competitive inhibition i Problems and theory. Arch Int Pharmacodyn Ther 99(1):32–49
16. Dierynck I, De Wit M, Gustin E, Keuleers I, Vandersmissen J, Hallenberger S, Hertogs K (2007) Binding kinetics of darunavir to human immunodeficiency virus type 1 protease explain the potent antiviral activity and high genetic barrier. J Virol 81(24):13845–13851. https://doi.org/10.1128/jvi.01184-07
17. Hightower KE, Wang R, DeAnda F, Johns BA, Weaver K, Shen Y, Tomberlin GH, Carter HL III, Broderick T, Sigethy S (2011) Dolutegravir (S/GSK1349572) exhibits significantly slower dissociation than raltegravir and elvitegravir from wild-type and integrase inhibitor-resistant HIV-1 integrase-DNA complexes. Antimicrob Agents Chemother 55(10):4552–4559
18. Fierens FL, Vanderheyden PM, Roggeman C, Vande Gucht P, De Backer JP, Vauquelin G (2002) Distinct binding properties of the AT(1) receptor antagonist [(3)H]candesartan to intact cells and membrane preparations. Biochem Pharmacol 63(7):1273–1279. https://doi.org/10.1016/s0006-2952(02)00859-6
19. Le MT, Pugsley MK, Vauquelin G, Van Liefde I (2007) Molecular characterisation of the interactions between olmesartan and telmisartan and the human angiotensin II AT1 receptor. Br J Pharmacol 151(7):952–962. https://doi.org/10.1038/sj.bjp.0707323
20. Motulsky HJ, Mahan L (1984) The kinetics of competitive radioligand binding predicted by the law of mass action. Mol Pharmacol 25(1):1–9
21. Bosma R, Witt G, Vaas LAI, Josimovic I, Gribbon P, Vischer HF, Gul S, Leurs R (2017) The target residence time of antihistamines determines their antagonism of the G protein-coupled histamine H1 receptor. Front Pharmacol 8:667. https://doi.org/10.3389/fphar.2017.00667
22. Carboni L, Negri M, Michielin F, Bertani S, Fratte SD, Oliosi B, Cavanni P (2012) Slow dissociation of partial agonists from the D2 receptor is linked to reduced prolactin release. Int J Neuropsychopharmacol 15(5):645–656
23. Kati WM, Montgomery D, Carrick R, Gubareva L, Maring C, McDaniel K, Steffy K, Molla A, Hayden F, Kempf D, Kohlbrenner W (2002) In vitro characterization of A-315675, a highly potent inhibitor of A and B strain influenza virus neuraminidases and influenza virus replication. Antimicrob Agents Chemother 46(4):1014–1021. https://doi.org/10.1128/AAC.46.4.1014-1021.2002
24. Weiss M, Kang W (2004) Inotropic effect of digoxin in humans: mechanistic pharmacokinetic/pharmacodynamic model based on slow receptor binding. Pharm Res 21(2):231–236. https://doi.org/10.1023/b:pham.0000016236.36210.a6
25. Äbelö A, Gabrielsson J, Holstein B, Eriksson UG, Holmberg J, Karlsson MO (2001) Pharmacodynamic modelling of reversible gastric acid pump inhibition in dog and man. Eur J Pharm Sci 14(4):339–346
26. Abelö A, Andersson M, Holmberg AA, Karlsson MO (2006) Application of a combined effect compartment and binding model for gastric acid inhibition of AR-HO47108: a potassium competitive acid blocker, and its active metabolite AR-

HO47116 in the dog. Eur J Pharm Sci 29(2):91–101. https://doi.org/10.1016/j.ejps.2006.05.014
27. Yassen A, Olofsen E, Dahan A, Danhof M (2005) Pharmacokinetic-pharmacodynamic modeling of the antinociceptive effect of buprenorphine and fentanyl in rats: role of receptor equilibration kinetics. J Pharmacol Exp Ther 313(3):1136–1149
28. Yassen A, Kan J, Olofsen E, Suidgeest E, Dahan A, Danhof M (2006) Mechanism-based pharmacokinetic-pharmacodynamic modeling of the respiratory-depressant effect of buprenorphine and fentanyl in rats. J Pharmacol Exp Ther 319(2):682. https://doi.org/10.1124/jpet.106.107953
29. Yassen A, Olofsen E, Romberg R, Sarton E, Danhof M, Dahan A (2006) Mechanism-based pharmacokinetic-pharmacodynamic modeling of the antinociceptive effect of buprenorphine in healthy volunteers. Anesthesiology 104(6):1232–1242. https://doi.org/10.1097/00000542-200606000-00019
30. Yassen A, Olofsen E, Romberg R, Sarton E, Teppema L, Danhof M, Dahan A (2007) Mechanism-based PK/PD modeling of the respiratory depressant effect of buprenorphine and fentanyl in healthy volunteers. Clin Pharmacol Ther 81(1):50–58. https://doi.org/10.1038/sj.clpt.6100025
31. Wagner J (1968) Kinetics of pharmacologic response I Proposed relationships between response and drug concentration in the intact animal and man. J Theor Biol 20(2):173–201
32. Krzyzanski W, Jusko WJ (1998) Integrated functions for four basic models of indirect pharmacodynamic response. J Pharm Sci 87(1):67–72
33. Krzyzanski W, Jusko WJ (1998) Characterization of pharmacodynamic recession slopes for direct and indirect response models. J Pharmacokinet Biopharm 26(4):409–436
34. Van Liefde I, Vauquelin G (2009) Sartan–AT1 receptor interactions: in vitro evidence for insurmountable antagonism and inverse agonism. Mol Cell Endocrinol 302(2):237–243
35. Vanderheyden PM, Fierens FL, De Backer J, Vauquelin G (2000) Reversible and syntopic interaction between angiotensin receptor antagonists on Chinese hamster ovary cells expressing human angiotensin II type 1 receptors. Biochem Pharmacol 59(8):927–935. https://doi.org/10.1016/s0006-2952(99)00403-7
36. Verheijen I, Fierens FL, Debacker JP, Vauquelin G, Vanderheyden PM (2000) Interaction between the partially insurmountable antagonist valsartan and human recombinant angiotensin II type 1 receptors. Fundam Clin Pharmacol 14(6):577–585. https://doi.org/10.1111/j.1472-8206.2000.tb00443.x
37. Gleiter CH, Mörike KE (2002) Clinical pharmacokinetics of candesartan. Clin Pharmacokinet 41(1):7–17
38. Shibouta Y, Inada Y, Ojima M, Wada T, Noda M, Sanada T, Kubo K, Kohara Y, Naka T, Nishikawa K (1993) Pharmacological profile of a highly potent and long-acting angiotensin II receptor antagonist, 2-ethoxy-1-[[2'-(1H-tetrazol-5-yl) biphenyl-4-yl] methyl]-1H-benzimidazole-7-carboxylic acid (CV-11974), and its prodrug,(+/-)-1-(cyclohexyloxycarbonyloxy)-ethyl 2-ethoxy-1-[[2'-(1H-tetrazol-5-yl) biphenyl-4-yl] methyl]-1H-benzimidazole-7-carboxylate (TCV-116). J Pharmacol Exp Ther 266(1):114–120
39. Delacrétaz E, Nussberger J, Biollaz J, Waeber B, Brunner HR (1995) Characterization of the angiotensin II receptor antagonist TCV-116 in healthy volunteers. Hypertension 25(1):14–21
40. Reddy VP, Kozielska M, Johnson M, Vermeulen A, de Greef R, Liu J, Groothuis GM, Danhof M, Proost JH (2011) Structural models describing placebo treatment effects in schizophrenia and other neuropsychiatric disorders. Clin Pharmacokinet 50(7):429–450
41. Bialer M (1980) A simple method for determining whether absorption and elimination rate constants are equal in the one-compartment open model with first-order processes. J Pharmacokinet Biopharm 8(1):111–113. https://doi.org/10.1007/BF01059453
42. Church MK (2016) Allergy histamine and antihistamines Handb Exp Pharmaco. Springer International Publishing, Cham
43. Cuvillo Bernal AD, Mullol I Miret J, Bartra Tomàs J, Dávila I, Jáuregui I, Montoro J, Sastre J, Valero A (2006) Comparative pharmacology of the H1 antihistamines. J Investig Allergol Clin Immunol 16:3–12
44. Desager J-P, Horsmans Y (1995) Pharmacokinetic-pharmacodynamic relationships of H1-antihistamines. Clin Pharmacokinet 28(5):419–432
45. Leysen JE, Gommeren W, Janssen PF, Janssen PA (1991) Comparative study of central and peripheral histamine-H1 receptor binding in vitro and ex vivo of non-sedating antihistamines and of noberastine, a new agent. Drug Dev Res 22(2):165–178
46. Gillard M, Van Der Perren C, Moguilevsky N, Massingham R, Chatelain P (2002) Binding characteristics of cetirizine and levocetirizine to human H(1) histamine receptors: contribution of Lys(191) and Thr(194). Mol Pharmacol 61(2):391–399. https://doi.org/10.1124/mol.61.2.391
47. Church MK, Gillard M, Sargentini-Maier ML, Poggesi I, Campbell A, Benedetti MS (2009) From pharmacokinetics to therapeutics. Drug Metab Rev 41(3):455–474
48. Wood-Baker R, Emanuel M, Hutchinson K, Howarth P (1993) The time course of action of three differing doses of noberastine, a novel H1-receptor antagonist, on histamine-induced skin wheals and the relationship to plasma drug concentrations in normal human volunteers. Br J Clin Pharmacol 35(2):166
49. Vauquelin G (2016) Effects of target binding kinetics on in vivo drug efficacy: koff, kon and rebinding. Br J Pharmacol 173(15):2319–2334
50. Fierens F, Vanderheyden PM, De Backer JP, Vauquelin G (1999) Binding of the antagonist [3H]candesartan to angiotensin II AT1 receptor-transfected [correction of tranfected] Chinese hamster ovary cells. Eur J Pharmacol 367(2–3):413–422. https://doi.org/10.1016/s0014-2999(98)00965-0
51. Hoare SRJ, Fleck BA, Williams JP, Grigoriadis DE (2020) The importance of target binding kinetics for measuring target binding affinity in drug discovery: a case study from a CRF(1) receptor antagonist program. Drug Discov Today 25(1):7–14. https://doi.org/10.1016/j.drudis.2019.09.011
52. Gooljarsingh LT, Fernandes C, Yan K, Zhang H, Grooms M, Johanson K, Sinnamon RH, Kirkpatrick RB, Kerrigan J, Lewis T (2006) A biochemical rationale for the anticancer effects of Hsp90 inhibitors: slow, tight binding inhibition by geldanamycin and its analogues. PNAS 103(20):7625–7630
53. Napier C, Sale H, Mosley M, Rickett G, Dorr P, Mansfield R, Holbrook M (2005) Molecular cloning and radioligand binding characterization of the chemokine receptor CCR5 from rhesus macaque and human. Biochem Pharmacol 71(1–2):163–172. https://doi.org/10.1016/j.bcp.2005.10.024
54. Hoare SR (2021) The problems of applying classical pharmacology analysis to modern in vitro drug discovery assays: slow binding kinetics and high target concentration. SLAS Discov 26(7):835–850
55. Morrison JF, Walsh CT (1988) The behavior and significance of slow-binding enzyme inhibitors. Adv Enzymol Relat Areas Mol Biol 61:201–301. https://doi.org/10.1002/9780470123072.ch5
56. Mager DE, Jusko WJ (2001) General pharmacokinetic model for drugs exhibiting target-mediated drug disposition. J Pharmacokinet Pharmacodyn 28(6):507–532. https://doi.org/10.1023/a:1014414520282
57. Slater JW, Zechnich AD, Haxby DG (1999) Second-generation antihistamines. Drugs 57(1):31–47

58. Ramakrishnan R, DuBois DC, Almon RR, Pyszczynski NA, Jusko WJ (2002) Fifth-generation model for corticosteroid pharmacodynamics: application to steady-state receptor down-regulation and enzyme induction patterns during seven-day continuous infusion of methylprednisolone in rats. J Pharmacokinet Pharmacodyn 29(1):1–24. https://doi.org/10.1023/a:1015765201129
59. Black JW, Leff P (1983) Operational models of pharmacological agonism. Proc R Soc Lond B Biol Sci 220(1219):141–162
60. Vanderheyden PM, Verheijen I, Fierens FL, Backer JP, Vauquelin G (2000) Binding characteristics of [(3)H]-irbesartan to human recombinant angiotensin type 1 receptors. J Renin Angiotensin Aldosterone Syst 1(2):159–165. https://doi.org/10.3317/jraas.2000.020
61. Israili Z (2000) Clinical pharmacokinetics of angiotensin II (AT1) receptor blockers in hypertension. J Hum Hypertens 14(1):S73–S86
62. Li X, Mo E, Chen L (2022) Pharmacokinetics and bioequivalence evaluation of 2 olmesartan medoxomil and amlodipine besylate fixed-dose combination tablets in healthy Chinese volunteers under fasting and fed conditions. Clin Pharmacol Drug Dev. https://doi.org/10.1002/cpdd.1086
63. Church DS, Church MK (2011) Pharmacology of antihistamines. World Allergy Organ J 4(3 Suppl):S22-27. https://doi.org/10.1097/WOX.0b013e3181f385d9
64. Anthes JC, Gilchrest H, Richard C, Eckel S, Hesk D, West RE Jr, Williams SM, Greenfeder S, Billah M, Kreutner W, Egan RE (2002) Biochemical characterization of desloratadine, a potent antagonist of the human histamine H(1) receptor. Eur J Pharmacol 449(3):229–237. https://doi.org/10.1016/s0014-2999(02)02049-6
65. Meier E, Narvekar A, Iyer GR, DuBiner HB, Vutikullird A, Wirta D, Sall K (2017) Pharmacokinetics and safety of olopatadine hydrochloride 0.77% in healthy subjects with asymptomatic eyes: data from 2 independent clinical studies. Clin Ophthalmol. https://doi.org/10.2147/OPTH.S126690
66. Kwon O-S, Kim H-J, Pyo H, Chung S-J, Chung YB (2005) Determination of mequitazine in human plasma by gas-chromatography/mass spectrometry with ion-trap detector and its pharmacokinetics after oral administration to volunteers. Arch Pharm Res 28(10):1190–1195
67. Moulton BC, Fryer AD (2011) Muscarinic receptor antagonists, from folklore to pharmacology; finding drugs that actually work in asthma and COPD. Br J Pharmacol 163(1):44–52
68. Horhota ST, van Noord JA, Verkleij CB, Bour LJ, Sharma A, Trunk M, Cornelissen PJ (2015) In vitro, pharmacokinetic, pharmacodynamic, and safety comparisons of single and combined administration of tiotropium and salmeterol in COPD patients using different dry powder inhalers. AAPS J 17(4):871–880
69. Abernethy DR (1992) Pharmacokinetics and pharmacodynamics of amlodipine. Cardiology 80:31–36
70. Gossas T, Vrang L, Henderson I, Sedig S, Sahlberg C, Lindström E, Danielson UH (2012) Aliskiren displays long-lasting interactions with human renin. Naunyn Schmiedebergs Arch Pharmacol 385(2):219–224
71. Luft FC, Weinberger MH (2008) Antihypertensive therapy with aliskiren. Kidney Int 73(6):679–683. https://doi.org/10.1038/sj.ki.5002732
72. Boas RA, Villiger JW (1985) Clinical actions of fentanyl and buprenorphine the significance of receptor binding. Br J Anaesth 57(2):192–196. https://doi.org/10.1093/bja/57.2.192
73. Elkader A, Sproule B (2005) Buprenorphine. Clin Pharmacokinet 44(7):661–680
74. Hale JJ, Mills SG, MacCoss M, Finke PE, Cascieri MA, Sadowski S, Ber E, Chicchi GG, Kurtz M, Metzger J, Eiermann G, Tsou NN, Tattersall FD, Rupniak NMJ, Williams AR, Rycroft W, Hargreaves R, MacIntyre DE (1998) Structural optimization affording 2-(R)-(1-(R)-3, 5-bis (trifluoromethyl) phenylethoxy)-3-(S)-(4-fluoro) phenyl-4-(3-oxo-1, 2, 4-triazol-5-yl) methylmorpholine, a potent, orally active, long-acting morpholine acetal human NK-1 receptor antagonist. J Med Chem 41(23):4607–4614. https://doi.org/10.1021/jm980299k
75. Majumdar AK, Howard L, Goldberg MR, Hickey L, Constanzer M, Rothenberg PL, Crumley TM, Panebianco D, Bradstreet TE, Bergman AJ (2006) Pharmacokinetics of aprepitant after single and multiple oral doses in healthy volunteers. J Clin Pharmacol 46(3):291–300
76. Rittweger M, Arasteh K (2007) Clinical pharmacokinetics of darunavir. Clin Pharmacokinet 46(9):739–756
77. Boffito M, Jackson A, Amara A, Back D, Khoo S, Higgs C, Seymour N, Gazzard B, Moyle G (2011) Pharmacokinetics of once-daily darunavir-ritonavir and atazanavir-ritonavir over 72 hours following drug cessation. Antimicrob Agents Chemother 55(9):4218–4223
78. Abel S, Back DJ, Vourvahis M (2009) Maraviroc: pharmacokinetics and drug interactions. Antivir Ther 14(5):607–618
79. Davies BE (2010) Pharmacokinetics of oseltamivir: an oral antiviral for the treatment and prophylaxis of influenza in diverse populations. J Antimicrob Chemother. https://doi.org/10.1093/jac/dkq015
80. Bardsley-Elliot A, Plosker GL (2000) Nelfinavir Drugs 59(3):581–620
81. Crommentuyn KM, Mulder JW, Mairuhu AT, van Gorp EC, Meenhorst PL, Huitema AD, Beijnen JH (2004) The plasma and intracellular steady-state pharmacokinetics of lopinavir/ritonavir in HIV-1-infected patients. Antivir Ther 9(5):779–785
82. Khaliq Y, Gallicano K, Venance S, Kravcik S, Cameron DW (2000) Effect of ketoconazole on ritonavir and saquinavir concentrations in plasma and cerebrospinal fluid from patients infected with human immunodeficiency virus. Clin Pharmacol Ther 68(6):637–646
83. Mehandru S, Markowitz M (2003) Tipranavir: a novel non-peptidic protease inhibitor for the treatment of HIV infection. Expert Opin Investig Drugs 12(11):1821–1828
84. Flores MV, Strawbridge J, Ciaramella G, Corbau R (2009) HCV-NS3 inhibitors: determination of their kinetic parameters and mechanism. Biochim Biophys Acta 1794(10):1441–1448
85. Yamada I, Suzuki F, Kamiya N, Aoki K, Sakurai Y, Kano M, Matsui H, Kumada H (2012) Safety, pharmacokinetics and resistant variants of telaprevir alone for 12 weeks in hepatitis C virus genotype 1b infection. J Viral Hepat 19(2):e112–e119
86. Klibanov OM, Vickery SB, Olin JL, Smith LS, Williams SH (2012) Boceprevir: a novel NS 3/4 protease inhibitor for the treatment of hepatitis C. Pharmacotherapy 32(2):173–190
87. Cottrell ML, Hadzic T, Kashuba AD (2013) Clinical pharmacokinetic, pharmacodynamic and drug-interaction profile of the integrase inhibitor dolutegravir. Clin Pharmacokinet 52(11):981–994
88. Brainard DM, Wenning LA, Stone JA, Wagner JA, Iwamoto M (2011) Clinical pharmacology profile of raltegravir, an HIV-1 integrase strand transfer inhibitor. J Clin Pharmacol 51(10):1376–1402
89. Ramanathan S, Mathias AA, German P, Kearney BP (2011) Clinical pharmacokinetic and pharmacodynamic profile of the HIV integrase inhibitor elvitegravir. Clin Pharmacokinet 50(4):229–244
90. Wood ER, Truesdale AT, McDonald OB, Yuan D, Hassell A, Dickerson SH, Ellis B, Pennisi C, Horne E, Lackey K, Alligood KJ, Rusnak DW, Gilmer TM, Shewchuk L (2004) A unique structure for epidermal growth factor receptor bound to GW572016 (Lapatinib): Relationships among protein

conformation, inhibitor off-rate, and receptor activity in tumor cells. Cancer Res 64(18):6652–6659. https://doi.org/10.1158/0008-5472.Can-04-1168
91. Spector NL, Robertson FC, Bacus S, Blackwell K, Smith DA, Glenn K, Cartee L, Harris J, Kimbrough CL, Gittelman M (2015) Lapatinib plasma and tumor concentrations and effects on HER receptor phosphorylation in tumor. PLoS ONE 10(11):e0142845
92. Lewandowicz A, Tyler PC, Evans GB, Furneaux RH, Schramm VL (2003) Achieving the ultimate physiological goal in transition state analogue inhibitors for purine nucleoside phosphorylase. J Biol Chem 278(34):31465–31468
93. Major PP, Agarwal RP, Kufe DW (1981) Clinical pharmacology of deoxycoformycin. Blood 58(1):91–96
94. Kim YB, Kopcho LM, Kirby MS, Hamann LG, Weigelt CA, Metzler WJ, Marcinkeviciene J (2006) Mechanism of Gly-Pro-pNA cleavage catalyzed by dipeptidyl peptidase-IV and its inhibition by saxagliptin (BMS-477118). Arch Biochem Biophys 445(1):9–18. https://doi.org/10.1016/j.abb.2005.11.010
95. Boulton DW (2017) Clinical pharmacokinetics and pharmacodynamics of saxagliptin, a dipeptidyl peptidase-4 inhibitor. Clin Pharmacokinet 56(1):11–24
96. Wang A, Dorso C, Kopcho L, Locke G, Langish R, Harstad E, Shipkova P, Marcinkeviciene J, Hamann L, Kirby MS (2012) Potency, selectivity and prolonged binding of saxagliptin to DPP4: Maintenance of DPP4 inhibition by saxagliptin in vitro and ex vivo when compared to a rapidly-dissociating DPP4 inhibitor. BMC Pharmacol 12(1):1–11
97. de Leon J, Diaz FJ, Wedlund P, Josiassen RC, Cooper TB, Simpson GM (2004) Haloperidol half-life after chronic dosing. J Clin Psychopharmacol 24(6):656–660
98. Lindström E, Levander S (2006) Sertindole: efficacy and safety in schizophrenia. Expert Opin Pharmacother 7(13):1825–1834
99. Yeung P-F, Hubbard J, Korchinski E, Midha K (1993) Pharmacokinetics of chlorpromazine and key metabolites. Eur J Clin Pharmacol 45(6):563–569
100. Winans E (2003) Aripiprazole. Am J Health Syst Pharm 60(23):2437–2445
101. Kohout TA, Xie Q, Reijmers S, Finn KJ, Guo Z, Zhu YF, Struthers RS (2007) Trapping of a nonpeptide ligand by the extracellular domains of the gonadotropin-releasing hormone receptor results in insurmountable antagonism. Mol Pharmacol 72(2):238–247. https://doi.org/10.1124/mol.107.035535
102. Suzuki H, Uemura H, Mizokami A, Hayashi N, Miyoshi Y, Nagamori S, Enomoto Y, Akaza H, Asato T, Kitagawa T (2019) Phase I trial of TAK-385 in hormone treatment-naïve Japanese patients with nonmetastatic prostate cancer. Cancer Med 8(13):5891–5902
103. Sullivan SK, Hoare SR, Fleck BA, Zhu YF, Heise CE, Struthers RS, Crowe PD (2006) Kinetics of nonpeptide antagonist binding to the human gonadotropin-releasing hormone receptor: implications for structure-activity relationships and insurmountable antagonism. Biochem Pharmacol 72(7):838–849. https://doi.org/10.1016/j.bcp.2006.07.011
104. Struthers RS, Chen T, Campbell B, Jimenez R, Pan H, Yen SS, Bozigian HP (2006) Suppression of serum luteinizing hormone in postmenopausal women by an orally administered nonpeptide antagonist of the gonadotropin-releasing hormone receptor (NBI-42902). J Clin Endocrinol Metab 91(10):3903–3907
105. Näbauer M, Erdmann E (1987) Reversal of toxic and non-toxic effects of digoxin by digoxin-specific fab fragments in isolated human ventricular myocardium. Klin Wochenschr 65(12):558–561
106. Noel F, Fagoo M, Godfraind T (1990) A comparison of the affinities of rat (Na++ K+)-ATPase isozymes for cardioactive steroids, role of lactone ring, sugar moiety and KCl concentration. Biochem Pharmacol 40(12):2611–2616
107. Iisalo E (1977) Clinical pharmacokinetics of digoxin. Clin Pharmacokinet 2(1):1–16
108. Sykes DA, Bradley ME, Riddy DM, Willard E, Reilly J, Miah A, Bauer C, Watson SJ, Sandham DA, Dubois G (2016) Fevipiprant (QAW039), a slowly dissociating CRTh2 antagonist with the potential for improved clinical efficacy. Mol Pharmacol 89(5):593–605
109. Erpenbeck VJ, Vets E, Gheyle L, Osuntokun W, Larbig M, Neelakantham S, Sandham D, Dubois G, Elbast W, Goldsmith P (2016) Pharmacokinetics, safety, and tolerability of fevipiprant (QAW039), a novel CRTh2 receptor antagonist: results from 2 randomized, phase 1, placebo-controlled studies in healthy volunteers. Clin Pharmacol Drug Dev 5(4):306–313
110. Day RO, Graham GG, Hicks M, McLachlan AJ, Stocker SL, Williams KM (2007) Clinical pharmacokinetics and pharmacodynamics of allopurinol and oxypurinol. Clin Pharmacokinet 46(8):623–644. https://doi.org/10.2165/00003088-200746080-00001
111. Lovmar M, Tenson T, Mn E (2004) Kinetics of macrolide action: the josamycin and erythromycin cases. J Biol Chem 279(51):53506–53515
112. Periti P, Mazzei T, Mini E, Novelli A (1989) Clinical pharmacokinetic properties of the macrolide antibiotics. Clin Pharmacokinet 16(4):193–214. https://doi.org/10.2165/00003088-198916040-00001